

NJC

Accepted Manuscript



This is an *Accepted Manuscript*, which has been through the Royal Society of Chemistry peer review process and has been accepted for publication.

Accepted Manuscripts are published online shortly after acceptance, before technical editing, formatting and proof reading. Using this free service, authors can make their results available to the community, in citable form, before we publish the edited article. We will replace this *Accepted Manuscript* with the edited and formatted *Advance Article* as soon as it is available.

You can find more information about *Accepted Manuscripts* in the [Information for Authors](#).

Please note that technical editing may introduce minor changes to the text and/or graphics, which may alter content. The journal's standard [Terms & Conditions](#) and the [Ethical guidelines](#) still apply. In no event shall the Royal Society of Chemistry be held responsible for any errors or omissions in this *Accepted Manuscript* or any consequences arising from the use of any information it contains.



Journal Name

COMMUNICATION

Highly Porous Pd Nanostructures and Reduced Graphene Hybrids: Excellent Electrocatalytic Activity towards Hydrogen Peroxide†

Received 00th January 20xx,
Accepted 00th January 20xx

Subash Chandra Sahu,^a Tapan Kumar Behera,^a Ajit Dash,^a Bijayalaxmi Jena,^b Arnab Ghosh^c and Bikash Kumar Jena^{a*}

DOI: 10.1039/x0xx00000x

www.rsc.org/

A facile approach has developed for synthesis of highly porous Pd nanostructures (PPd NSs) and its graphene hybrid (RG-PPd NSs). The PPd NSs are well-dispersed on graphene support and retain their unique morphology. The RG-PPd NSs modified electrode shows high sensitivity towards H₂O₂ without the usage of redox mediator/enzyme.

In the recent years, palladium nanostructures (Pd NSs) have been receiving intense research interest. They find their wide and potential application in catalysis, electrocatalysis, reduction of environmental pollutants, fabrication of sensor and biosensors.^{1,2} These have been favored as an alternative to platinum because of low cost and high resistance to surface poisoning.^{3,4} Previous reports have demonstrated that the catalytic properties are governed by the size, shape and surface morphology.⁵⁻⁷ In the past few decades, Pd NSs of various shapes and well-defined structures such as nanowire, nanorod, nanocube, and nanosheets etc. have been successfully synthesized.^{8,9}

The Pd nanoparticles with porous structures, rough surface, and dendritic morphology have been attracting towards fuel cell and sensor applications because of their superior performance in catalysis and electrocatalysis.¹⁰ The enhanced activity of these materials is believed to be due to the presence of high index facets, highly active surface atoms, rich edge and corner atoms, etc.¹⁰ Recently, efforts have been dedicated to the synthesis of Pd NPs with porous structures. The porous structures provide large surface area and allow the utilization of maximum atoms in the catalytic process.¹¹ Several methods have been documented for the preparation of porous Pd NSs.¹²⁻¹⁶ However, these methods adopt complicated process, the use of toxic reducing agents, the organic medium and long duration of reaction time.¹²⁻¹⁶

Therefore, a simple, rapid, one pot and seedless synthesis of porous Pd NSs is highly desirable and technically important. In the present communication, we report a facile, rapid and bio-friendly method for the synthesis of highly porous Pd NSs in the aqueous medium within 45 min of reaction. Rutin, a biomolecule known as vitamin P has been employed as reducing/stabilizing agent.

For the improvement of the performance, metal nanoparticles as catalysts have been immobilized on the catalytic support.¹⁷ It has been reported that catalytic support should possess high electrical conductivity, good chemical inertness and large surface area.¹⁸ As a new carbon-based support, graphene has been treated as an ideal catalytic support owing to its vast surface area, good electrical conductivity, and high chemical/thermal inertness.¹⁹ The graphene supported spherical shaped Pd nanoparticles has been successfully synthesized.^{20,21} However, there is a limited report available on the synthesis of graphene decorated with anisotropic Pd nanostructures.^{22,23} It is very difficult to retain the shape, morphology and surface structure of metal nanoparticle on graphene surface.²⁴ Therefore, substantial efforts have been made to the synthesis of graphene-metal nanostructures with unique morphology by different approaches.²⁵ As far as our knowledge, no such report portrays the synthesis of graphene supported Pd nanostructures with porous morphology. Here, we developed a facile ex-situ approach for the synthesis of reduced graphene and highly porous Pd nanostructures hybrids and studied their electrocatalytic activity towards H₂O₂. It is worth to point here that this is the first report depicting the synthesis and electrocatalytic activity of graphene supported Pd nanostructures with a unique porous feature.

The synthesis of metal nanostructures with porous morphology is highly difficult and requires specific structure regulating and capping agents. Utilizing a bio-friendly molecule, rutin, we developed a facile approach for the synthesis of highly porous Pd NSs in an aqueous medium. Fig.1 shows the TEM images of the PPd NSs at different magnifications. The TEM images evidently indicate that the

^a Colloids and Materials Chemistry Department, CSIR-Institute of Minerals and Materials Technology, Bhubaneswar, Odisha, India. Fax: 0674-2581637 Tel: 0674-2379410.

^b Department of Chemistry, Utkal University, Bhubaneswar, Odisha, India.

^c Institute of Physics, Bhubaneswar, Odisha, India.

* Corresponding Author; Email: bikash@imtm.res.in

resulting synthetic condition produced high yield of Pd NSs with impressive porous structure and distinctly rough surface. It reveals that each PPd NS consists of numerous nano entities that are interconnected and arranged to form an enormous number of pores throughout the nanostructure. The average diameter/size of PPd NSs is estimated ~ 38 nm. From the high-resolution TEM image (Fig.1F), the lattice fringe width of porous PPd NSs was estimated to be 2.24 Å corresponding to the (111) planes of the face centered cubic (fcc) Pd. The surface composition of PPd NSs was verified by XPS analysis (Fig.1G). The XPS spectrum of PPd NSs exhibits two prominent peaks at 335.09 eV and 340.15 eV corresponding to the binding energies (BE) for $3d_{5/2}$ and $3d_{3/2}$ of elemental Palladium.

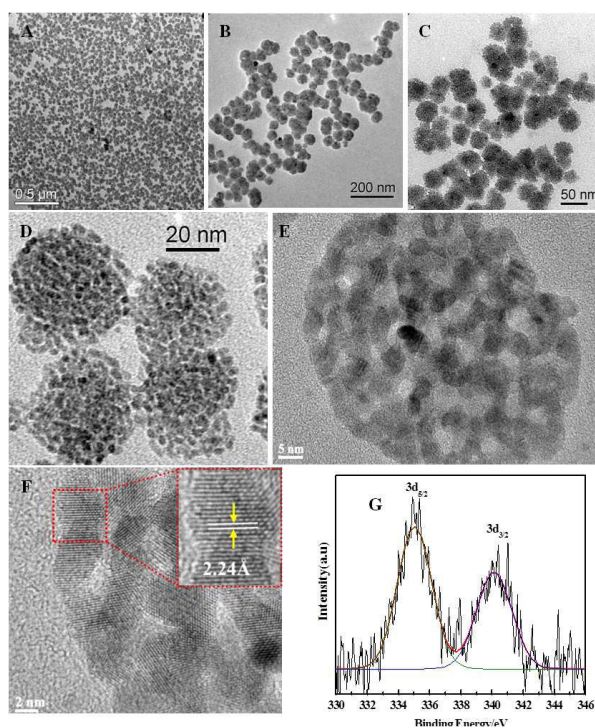


Fig. 1 (A-F) TEM images and (G) XPS spectrum (Pd 3d) of PPd NSs.

The graphene supported PPd NSs hybrids (RG-PPd NSs) was synthesized by ex-situ reduction of GO in the presence of colloidal PPd NSs (Fig 2, scheme). The GO was synthesized by the modified Hummer's method (See ESI[†]). The as-synthesized RG-PPd NSs was characterized with the TEM technique (Fig. 2 A and B). It reveals that the PPd NSs are well distributed on the surface of graphene and retained its porous morphology. The reduction of GO during the formation of RG-PPd NSs was clarified by UV-visible, Raman and XPS measurements. The UV-visible spectrum of GO (Fig. 2C red trace), exhibit one major absorbance peak at 228 nm and shoulder peak at 290 nm. This observation reveals the $\pi-\pi^*$ and $n-\pi^*$ electronic transitions of the functional groups C=C and C=O present in GO, respectively.²⁶ However, only one absorbance peak at 260 nm was observed for RG-PPd NSs (Fig.2C black trace) indicating

the reduction of GO and increase in extending conjugation.²⁷ The optical images of GO and RG-PPd NSs (Fig.2C inset) further indicates the reduction of GO to graphene. The aqueous solution of GO is a yellowish brown color solution. However, the color of the solution slowly changes to black during the synthesis of RG-PPd NSs. Raman spectroscopy is a potential technique to characterize the carbon-based materials.²⁸ It has been widely applied to detect various defects, impurity, and the number of layers in graphene-based materials. In the Raman spectra (Fig.2D red trace), GO exhibits two

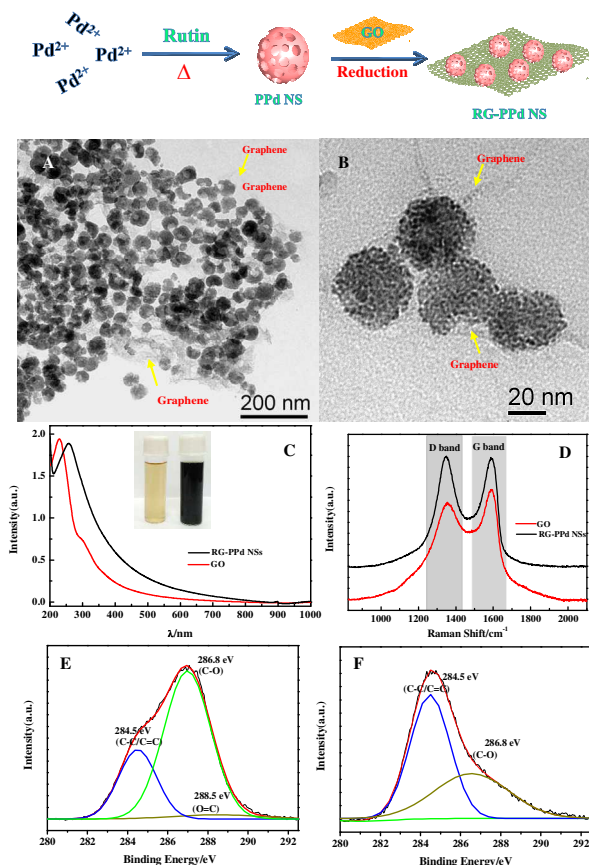


Fig. 2 Scheme showing the procedure for synthesis of RG-PPd NSs. TEM images (A,B) of RG-PPd NSs, UV-vis absorption (C), Raman (D) spectra of GO (red trace) and RG-PPd NSs (black trace) and C1s XPS spectra of GO (E) and RG-PPd NSs(F). The inset of Figure 2C shows the optical images of GO (yellowish brown color) and RG-PPd NSs (black color)

characteristic peaks at 1355 cm^{-1} (D band) and 1589 cm^{-1} (G band).²⁹ After the formation of RG-PPd NSs (Fig.2D black trace), the intensity of D to G band (I_D/I_G) increases as compared to that of GO.³⁰ These results suggest the formation of numerous small size and new graphitic (sp^2) domains indicating the efficient reduction of GO.³⁰ This fact is further supported by the analysis of C1s XPS spectra of GO and RG-PPd NSs (Fig.2 E and F). The C1s spectrum of GO exhibits two major peaks at the binding energies of 284.5 eV and 286.8 eV and a

weak peak at 288.5 eV. These peaks are assigned to the functional groups C-C/C=C, C-O and C=O, respectively.¹⁸ Interestingly, the RG-PPd NSs shows a predominant peak related to the BE of C-C/C=C bond and the weaker peaks for the BE of carbon-oxygen functional groups. This observation indicates the removal of oxygen functional groups in RG-PPd NSs.³¹ Thus, the results from UV-vis, Raman and XPS analysis confirm the efficient reduction of GO to RG after the formation of RG-PPd NSs.

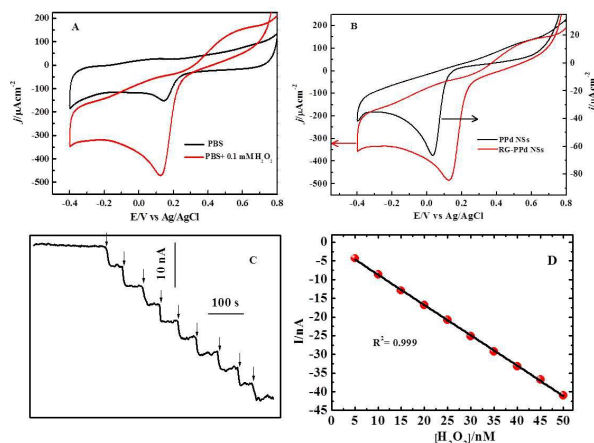


Fig. 3 (A) CVs of RG-PPd NSs modified electrode in 0.1M PBS solution (pH=7.4) in the absence (black trace) and presence (red trace) of 0.1 mM H_2O_2 . (B) CVs of RG-PPd NSs (red trace) and PPd NSs (black trace) modified electrode in 0.1M PBS solution containing 0.1 mM H_2O_2 , (C) Amperometric (*i*-*t*) response of RG-PPd NSs modified electrode towards successive injection of 5 nM H_2O_2 , (D) corresponding calibration plot.

Inspired by the unique porous structure of PPd NSs and attractive properties of graphene, the electrocatalytic activity towards H_2O_2 has been studied. Fig.3 shows the cyclic voltammetric response of RG-PPd NSs towards H_2O_2 in 0.1 M phosphate buffer solution (PBS). In the absence of H_2O_2 (Fig.3C black trace), the RG-PPd NSs electrode shows a reduction peak at +0.145 V corresponds to the reduction of palladium oxide in neutral PBS solution. Interestingly, in the presence of H_2O_2 (Fig.3C red trace) the reduction current increased enormously. This observation confirms that the RG-PPd NSs electrode catalyses the reduction of H_2O_2 . Further, the catalytic performance of RG-PPd NSs electrode has been compared with PPd NSs modified electrode to draw the effect of graphene support. Fig.3B shows the cyclic voltammetric behavior of RG-PPd NSs (red trace) and PPd NSs (black trace) modified electrodes. The RG-PPd NSs electrode exhibits a current density of 445.267 μAcm^{-2} that is 7.24 times higher than that of PPd NSs electrode. Further, the RG-PPd NSs electrode reduces the H_2O_2 at a potential of 0.126 V, which is 92.3 mV less over potential as compared to that of PPd NSs electrode (0.034 V). This result indicates that the RG-PPd NSs effectively catalyses the reduction of H_2O_2 . The excellent catalytic performance of RG-PPd NSs may be ascribed to the (a) high conductivity of graphene enhancing the rate of

electron transfer process, (b) large surface area of graphene supporting to the well dispersion of PPd NSs and avoiding their aggregation, and (c) the synergistic effect of graphene and the interesting porous morphology of PPd NSs playing the vital role in the electrocatalytic process.

The amperometric technique is the most efficient strategy to investigate the real current efficiency in the electrocatalytic property of the nanomaterials. Fig 3C illustrates the current constant potential amperometry (*i*-*t*) profile for RG-PPd NSs modified electrode upon successive addition of 5 nM H_2O_2 in 0.1 M PBS. The potential was held at the reduction potential of H_2O_2 . It can be observed from *i*-*t* curve that the RG-PPd NSs electrode rapidly response 5 nM H_2O_2 with a very fast response time (< 3s). The RG-PPd NSs modified transducer can effectively monitor very low concentration down to 5 nM without using any redox mediator and peroxidase enzymes. Such low concentration sensing of the present transducer is worth comparing with the supported Pd nanomaterials based various non-enzymatic and enzymatic sensors such as electrochemically reduced graphene oxide/Amino-thiophenol/Pd nanoparticle (0.016 μM), graphene/hollow Ag-Pd alloy nanoparticle (1.4 μM), Pd nanoparticle/graphene nanosheet (0.05 μM), hollow Au-Pd alloy nanoparticle/nitrogen doped graphene (0.02 μM), Pd nanoparticle/Thiolated graphene oxide (0.22 μM), Polyethylenimine/graphene oxide/Pd particles (0.2 μM), Palladium nanoparticles/carbon nanofiber (0.1 μM) and Pd nanoparticle/mesoporous carbon nanospheres (1.0 μM).³²⁻⁴⁰ The RG-PPd NSs electrode linearly responded the concentration of H_2O_2 (Fig.3D) and the sensitivity of the present electrode was estimated to be 0.81 nA/nM. The low detection limit of the present electrode was estimated to be 1 nM ($S/N \geq 3$). Further works are underway to explore more on the selectivity, stability and validation in real sample analysis for practical application.

In summary, we developed a facile approach for the rapid synthesis of highly porous Pd nanostructures without using any seed, toxic organic reagents and sophisticated strategy. Further, the as-prepared Porous Pd NSs were successfully loaded on the surface of reduced graphene oxide by an ex-situ approach. The synergistic effect and extraordinary properties of graphene and porous structure of Pd enhanced the catalytic performance of RG-PPd NSs towards the reduction of H_2O_2 . The RG-PPd NSs showed fast response time, high sensitivity, very low limit of detection. Therefore, the electrochemical analysis indicated the RG-PPd NSs as the promising nanostructured platform for the fabrication of electrochemical sensors.

Experimental

Porous Pd nanoparticles were synthesized by reducing the PdCl_2 solution by rutin hydrate. In particular, 10 ml of 0.3 mM aqueous PdCl_2 solution was taken in the three-necked round bottom flask. Then, the solution was heated to boiling to 100 $^\circ\text{C}$ and at the same condition 0.6 ml of 15 mM rutin solution was added rapidly. The reaction was allowed to continue for

45 minutes. The as-prepared Pd nanostructures were washed with distilled water repeatedly and stored in a cool and dry place for prior use.

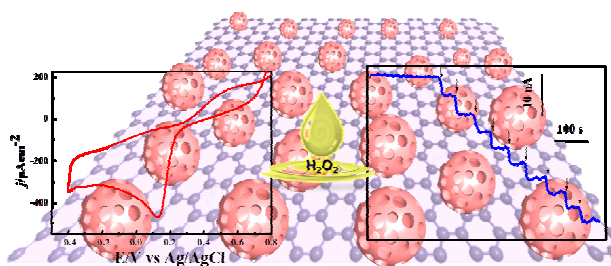
Graphene supported porous Pd nanostructures were synthesized by a facile ex-situ method. In brief, 1 mg of GO was well dispersed in 10 ml of distilled water. Then, 10 ml of the colloidal solution of as-synthesized porous Pd nanostructures was added to the GO solution and sonicated for 30 minutes. Finally, 1 ml aqueous solution of 50 mM NaBH₄ was added dropwise to the mixture with continuous stirring. The reaction mixture was left undisturbed for 30 min and gradually change of the color from yellow to black was observed.

Acknowledgements

The authors are grateful to Prof. B.K. Mishra, Director, CSIR-IMMT for the constant support and permission to carry out this work. BKJ acknowledge CSIR Project (YSP-02, P-81-113) and MULTIFUN (CSC-0101), BRNS, Mumbai, India (No.2013/37p/67/BRNS) and MNRE, New Delhi, India (No.102/87/2011-NT) for financial support. The Authors are thankful to Prof. P. V. Satyam, Institute of Physics, Bhubaneswar for TEM measurement.

Notes and references

- 1 C. Deraedt and D. Astruc, *Acc. Chem. Res.*, 2014, **47**, 494.
- 2 C. Bianchini and P.K. Shen, *Chem. Rev.*, 2009, **109**, 4183.
- 3 E. Antolini, *Energy Environ. Sci.*, 2009, **2**, 915.
- 4 B.K. Jena, S.C. Sahu, B. Satpati, R.K. Sahu, D. Behera and S. Mohanty, *Chem. Commun.*, 2011, **47**, 3796.
- 5 M. Shao, J. Odell, M. Humbert, T. Yu and Y. Xia, *J. Phys. Chem. C*, 2013, **117**, 4172.
- 6 J. Chen, Q. Zhang, Y. Wang and H. Wan, *Adv. Synth. Catal.*, 2008, **350**, 453.
- 7 D. Gao, H. Zhou, J. Wang, S. Miao, F. Yang, G. Wang, J. Wang and X. Bao, *J. Am. Chem. Soc.*, 2015, **137**, 4288.
- 8 Y. Xiong and Y. Xia, *Adv. Mater.*, 2007, **19**, 3385.
- 9 A. R. Tao, S. Habas and P. Yang, *Small*, 2008, **4**, 310.
- 10 B. Lim and Y. Xia, *Angew. Chem. Int. Ed.*, 2011, **50**, 76.
- 11 W. Hong, Y. Fang, J. Wang and E. Wang, *J. Power Sources*, 2014, **248**, 553.
- 12 F. Wang, C. Li, L.-D. Sun, C.-H. Xu, J. Wang, J.C. Yu and C.-H. Yan, *Angew. Chem. Int. Ed.*, 2012, **51**, 4872.
- 13 G. Fu, W. Han, L. Yao, J. Lin, S. Wei, Y. Chen, Y. Tang, Y. Zhou, T. Lu and X. Xia, *J. Mater. Chem.*, 2012, **22**, 17604.
- 14 S. Tang, S. Vongehr, Z. Zheng, H. Ren and X. Meng, *Nanotechnology*, 2012, **23**, 255606.
- 15 Q. Gao, M.R. Gao, J.W. Liu, M.Y. Chen, C.H. Cui, H.H. Li and S.H. Yu, *Nanoscale*, 2013, **5**, 3202.
- 16 X. Huang, Y. Li, Y. Chen, E. Zhou, Y. Xu, H. Zhou, X. Duan, Y. Huang, *Angew. Chem. Int. Ed.*, 2013, **52**, 2520.
- 17 Z. Zhang, J. Liu, J. Gu, L. Su and L. Cheng, *Energy Environ. Sci.*, 2014, **7**, 2535.
- 18 S.C. Sahu, A.K. Samantara, A. Dash, R. R. Juluri, R.K. Sahu, B. K. Mishra and B.K. Jena, *Nano Res.*, 2013, **6**, 635.
- 19 A. K. Geim and K. S. Novoselov, *Nat. Mater.*, 2007, **6**, 183.
- 20 S. Yang, J. Dong, Z. Yao, C. Shen, X. Shi, Y. Tian, S. Lin and X. Zhang, *Sci. Rep.*, 2014, **4**, 4501.
- 21 Y.-X. Huang, J.-F. Xie, X. Zhang, L. Xiong and H.-Q. Yu, *ACS Appl. Mater. Interfaces*, 2014, **6**, 15795.
- 22 C. Du, Y. Liao, X. Hua, W. Luo, S. Chen and G. Cheng, *Chem. Commun.*, 2014, **50**, 12843.
- 23 G. Fu, L. Tao, M. Zhang, Y. Chen, Y. Tang, J. Lin and T. Lu, *Nanoscale*, 2013, **5**, 8007.
- 24 T. Jin, S. Guo, J. Zuo and S. Sun, *Nanoscale*, 2013, **5**, 160.
- 25 J. Chai, F. Li, Y. Hu, Q. Zhang, D. Han and L. Niu, *J. Mater. Chem.*, 2011, **21**, 17922.
- 26 D. Li, M. B. Muller, S. Gilje, R. B. Kaner and G.C. Wallace, *Nat. Nanotechnol.*, 2008, **3**, 101.
- 27 J. Zhang, H. Yang, G. Shen, P. Cheng, J. Zhang and S. Guo, *Chem. Commun.*, 2010, **46**, 1112.
- 28 S.-S. Li, J.-J. Lv, Y.-Y. Hu, J.-N. Zheng, J.-R. Chen, A.-J. Wang and J.-J. Feng, *J. Power Sources*, 2014, **247**, 213.
- 29 S. Stankovich, D. A. Dikin, R. D. Piner, K. A. Kohlhaas, A. Kleinhammes, Y. Jia, Y. Wu, S. T. Nguyen and R. S. Ruoff, *Carbon*, 2007, **45**, 1558.
- 30 S. Mayavan, J.-B. Sim, S.-M. Choi, *J. Mater. Chem.*, 2012, **22**, 6953.
- 31 S.C. Sahu, A.K. Samantara, B. Satpati, S. Bhattacharjee and B.K. Jena, *Nanoscale*, 2013, **5**, 11265.
- 32 J.-M. You, D. Kim, S.K. Kim, M.-S. Kim, H.S. Han and S. Jeon, *Sens. Actuator B*, 2013, **178**, 450.
- 33 M.-M. Liu, W.-T. Wei, Y.-Z. Lu, H.-B. Wu and W. Chen, *Chin. J. of Anal. Chem.*, 2012, **40**, 1477.
- 34 X. Chen, Z. Cai, Z. Huang, M. Oyama, Y. Jiang and X. Chen, *Electrochim. Acta*, 2013, **97**, 398.
- 35 L. Shang, B. Zeng and F. Zhao, *ACS Appl. Mater. Interfaces*, 2015, **7**, 122.
- 36 J.-M. You, D. Kim and S. Jeon, *J. Nanosci. Nanotechnol.*, 2012, **12**, 3943.
- 37 C. Xu, L. Zhang, L. Liu, Y. Shi, H. Wang, X. Wang, F. Wang, B. Yuan and D. Zhang, *J. Electroanal. Chem.*, 2014, **731**, 67.
- 38 J. Huang, D. Wang, H. Hou and T. You, *Adv. Funct. Mater.*, 2008, **18**, 441.
- 39 D. Liu, Q. Guo, X. Zhang, H. Hou and T. You, *J. Colloid Interface Sci.*, 2015, **450**, 168.
- 40 X. Bian, K. Guo, L. Liao, J. Xiao, J. Kong, C. Ji and B. Liu, *Talanta* 2012, **99**, 256.

Table of Contents (TOC):

A new approach has been developed for highly porous Pd nanostructure-graphene hybrids as efficient electrocatalyst towards oxidation of H_2O_2